Supporting Information for

Entropic Trapping of DNA with a Nanofiltered Nanopore

Michelle H. Lam[†ǂ], Kyle Briggs[†ǂ], Konstantinos Kastritis[§ǂ], Martin Magill[§], Gregory R. Madejski[‡], James L. McGrath[‡], Hendrick W. de Haan*[§], and Vincent Tabard-Cossa*[†]

[†] Department of Physics, University of Ottawa, Ottawa, ON, Canada

[‡] Department of Biomedical Engineering, University of Rochester, Rochester, NY, USA

[§] Faculty of Science, University of Ontario Institute of Technology, Oshawa, ON, Canada

[ǂ] These authors contributed equally to this manuscript

*Corresponding Authors: Vincent Tabard-Cossa: tcossa@uOttawa.ca (experiment); Hendrick W. de Haan: Hendrick.deHaan@uoit.ca (simulation).

Table of Contents

Supporting Information Section S1: Simulation Setup

Simulations were used to study the motion of 1.2 kbp DNA in the diffusive mode of operation of the device. An effective multiscale approach was used. In the bulk of the cavity, the DNA was modelled by a single effective particle representing the center of mass of the polymer, and its diffusion was simulated using Brownian dynamics (BD). This model is justified where the dynamics occur on length scales much larger than the radius of gyration of the molecule. Near the filter, however, the dynamics of the entire polymer chain become important and a Brownian particle cannot faithfully model the polymer. In this region, the DNA was modelled as a wormlike chain, coarse-grained Langevin dynamics (CGLD) was used to simulate its motion. In the following sections we provide more detail on the simulations.

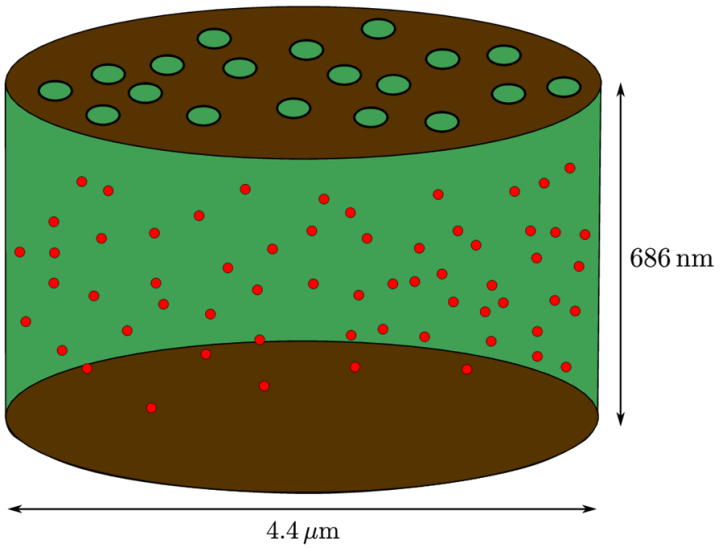

Figure S1: Schematic of the geometry used for the Brownian dynamics simulations. The effective dimensions for the gap height and cavity diameter are shown. The nominal dimensions for the cavity diameter and gap height were 4.5 μm and 800 nm respectively. The red dots represent the Brownian particles. To account for the fact that modelled polymers are treated as extended object, twice the radius of gyration, $2R_g$ ($R_g \approx 57$ nm), was subtracted from each of the dimensions resulting in a cavity diameter of 4.4 μm and a gap height of 686 nm.

Modelling the dynamics far from the filter

Polymer model

To carry out the simulation we used the HOOMD-blue molecular dynamics software package. Far from the filter we only considered the center of mass (COM) motion of the polymer. We modelled the COM as a single particle whose time evolution is given by Brownian dynamics (BD):

$$\dot{\vec{x}} = \sqrt{2D}\vec{\xi}(t), \tag{1}$$

where D is the diffusion coefficient and $\vec{\xi}(t)$ is a Gaussian random noise function. This model has a single free parameter, the diffusion coefficient. We expressed lengths in the BD simulations in units of nanometers (nm), and fixed the diffusion coefficient to be

$$D_{sim} = 1\frac{\mathrm{nm}^2}{\tau_{\mathrm{BD}}}, \tag{2}$$

where τ_{BD} is the simulation unit of time. Experimentally measured diffusion coefficients were used to determine the equivalent value of τ_{BD} in seconds. For a given experimental diffusion coefficient $D_{exp}(L_c)$ (which generally depends on the contour length, L_c), we set

$$1\frac{\mathrm{nm}^2}{\tau_{\mathrm{BD}}} = D_{sim} = D_{exp} = D_{exp}(L_c)\frac{\mathrm{nm}^2}{s}, \tag{3}$$

from which we determine

$$\tau_{\mathrm{BD}} = \frac{1}{D_{exp}(L_c)}s. \tag{4}$$

The numerical values of the diffusion coefficient were obtained from Petrov *et al*[1].

In order to probe the long times present in the experiment the time step was set to $\Delta t = 10\tau$. This choice of time step sets the mean jump size to be $\Delta x \approx 4$ nm, a value which is reasonable far from the filter as it is much smaller than even the smallest length in the device which stands at ≈ 700 nm (Figure S1).

Geometry

Figure S1 shows the geometry of the device assumed for the simulations described in this section. The nominal dimensions of the device were 4.5 μm and 800 nm for the cavity diameter and gap height respectively. To account for the fact that a polymer is an extended object we subtracted $2R_g$ ($R_g \approx 57$ nm) from each of the dimensions resulting in a cavity diameter of 4.4 μm and a gap height of 686 nm. The cavity walls were modelled as reflecting boundaries, with the trajectory of a particle that would cross the wall being reflected back into the cavity.

For the sensing pore membrane we assumed that the molecules cannot escape back into the loading well and thus modelled it as a reflecting boundary similar to the cavity walls. As such, the sensing pore itself was not explicitly incorporated in the boundary condition. However, the location of the sensing pore, which we assumed to be at the center of the membrane, dictated the initial condition for the particles in the simulation. The nanofilter membrane was treated as a special boundary condition described in the next subsection.

Interactions with the filter pores

As the dynamics near the filter are more complicated than simple diffusion in the bulk of the cavity, the results of the more detailed CGLD simulations were coupled to the BD simulations via a special boundary condition. The majority of the filter membrane was modelled as a reflecting

boundary with certain locations on its surface being absorbing windows, representing pores in an otherwise impermeable membrane. Upon interaction with an absorbing window a particle has a probability of escaping through the filter. The details of obtaining the probability of escape through a filter pore are discussed in the next section.

A randomly generated nanofilter was used in order to account for the inherent variability in the filter pore distribution. The absorbing windows were placed iteratively. Trial pore locations were drawn uniformly with the criteria that the window corresponding to any new pore has an edge-to-edge distance of at least 20 nm from any existing window. In addition, the center of all pores was required to be at least one pore radius away from the edge of the membrane. Pore locations that did not meet these criteria were discarded.

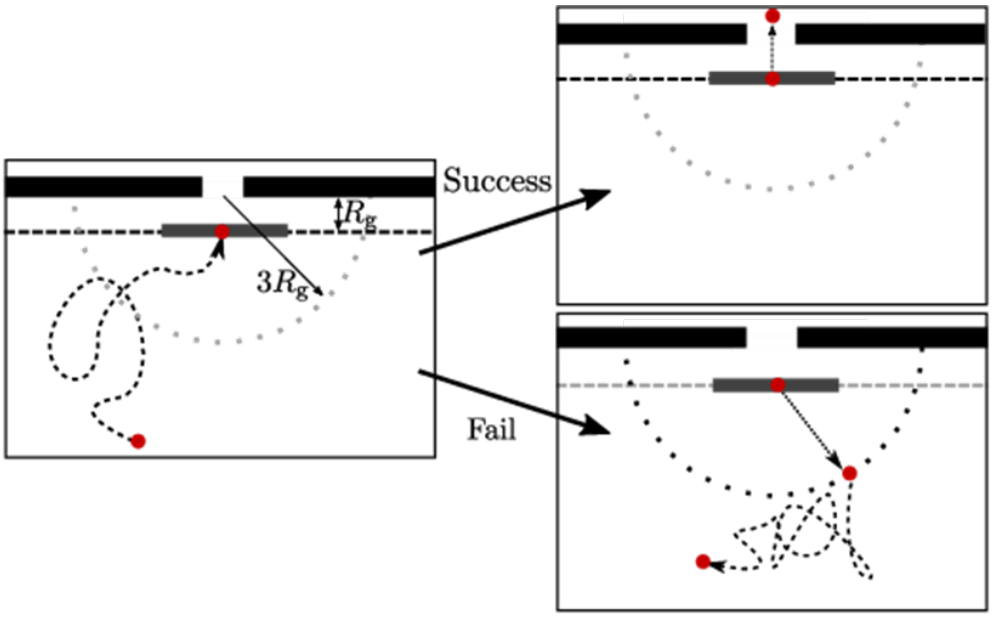

Figure S2: Schematic of the filter interaction for the Brownian particles. The grey rectangle represents a cross section of the disk of interaction for the pore. The black dashed line represents the excluded region of R_g from the pore. The black dotted line represents the rejection radius at $3R_g$.

Simulation procedure

We implicitly modelled the loading of the molecules into the cavity by initializing two thousand non-interacting particles into the cavity at a distance of R_g from the center of the sensing pore membrane. The simulations were run for 30 seconds according to the time mapping described in the previous subsection. For each filter pore size a total of ten different filter configurations were sampled.

As shown in Figure S2, a particle is determined to be near a filter pore in the boundary when it lies inside a disk with origin at the central axis of the pore and radius equal to two times the pore radius, displaced a distance R_g axially from the nanofilter pore. Upon interaction of a particle with a pore on the filter a random number is drawn, and if it less than the probability obtained from CGLD the particle successfully translocates. If not, it is returned to the bulk of the cavity by being placed at a random location on a hemisphere $3R_g$ radially away from the center of the nominal pore.

We modelled the recapture of molecules implicitly by assuming that all polymers remaining in the cavity at the end of the simulation would be successfully recaptured. The probability of recapture shown in Figure 3e of the main text was computed as

$$P_\tau(t) = 1 - \frac{N_{escaped}}{N_{initialized}} \tag{5}$$

Modelling the dynamics near the filter

Polymer model

As mentioned in the preceding section, near the nanofilter the DNA was modelled using a wormlike chain comprised of *N* identical monomers. To model the time evolution of the polymeric chain we used coarse-grained Langevin dynamics (CGLD)[2] in which monomers are taken to be spheres that experience Stokes drag and whose solvent interactions are implicit. The equation of motion for CGLD is

$$m\ddot{\vec{x}} = -\sum_i \nabla U_i(\vec{x}) - \xi\dot{\vec{x}} + \sqrt{2\xi k_B T}\vec{\xi}(t), \tag{6}$$

where ξ is the drag coefficient and $k_B T$ is the thermal energy. The fluctuation term $\vec{\xi}(t)$ is a random noise function that implicitly models thermal fluctuations in the solvent and satisfies

$$\langle\vec{\xi}(t)\rangle = 0, \tag{7}$$

$$\langle\xi_i(t)\xi_j(t')\rangle = \delta_{ij}\delta(t-t'). \tag{8}$$

The gradient term is the sum of all external forces. To evolve the equation in time we used the HOOMD-blue molecular dynamics package.

Bonds between pairs of adjacent monomers were modelled using the finitely extensible non-linear elastic potential,

$$U_{FENE}(r) = -\frac{1}{2}kr_{max}^2 \ln\left(1 - \frac{r^2}{r_{max}^2}\right). \tag{9}$$

The constants k and r_{max} represent the stiffness and the maximum possible extension of the bond respectively, with r being the center to center distance between monomers. The excluded volume interaction between monomers was modelled using the Weeks-Chandler-Anderson (WCA) potential,

$$U_{WCA}(r) = \begin{cases} 4\varepsilon[\left(\frac{\sigma}{r}\right)^{12} - \left(\frac{\sigma}{r}\right)^{6} + \varepsilon, & r < r_c \\ 0, & r \geq r_c \end{cases} \quad (10)$$

where ε is the interaction energy, σ the monomer diameter and $r_c = 2^{\frac{1}{6}}\sigma$ the cut-off distance.

To model the rigidity inherent to the DNA we used a three-body harmonic potential,

$$U_{angle}(\theta) = \frac{1}{2}k_{angle}\theta^2, \quad (11)$$

where k_{angle} is the stiffness of the spring and θ is the angle formed between three consecutive monomers along the chain.

The simulations used a self-consistent set of units with energy, mass, and distance as fundamental units. All other units were derived from these. The unit of energy was chosen to be the thermal energy k_BT with the units of length and mass chosen as the particle size σ and mass m respectively.

The units of time in this system are given by $\tau = \sigma\sqrt{\frac{m}{k_BT}}$. In accordance with Grest *et al*.,[3] the parameters of the FENE potential were chosen to be $k = 30\frac{k_BT}{\sigma^2}$ and $r_{max} = 1.5\sigma$. The persistence length of the polymer is $l_p \approx \frac{k_{angle}}{k_BT}\sigma$,[4] so that changing the stiffness of the angle bond changes the persistence length.

We set the correspondence between simulation lengths and experimental lengths by choosing the effective monomer diameter, σ, to equal 5 nm. The persistence length of the polymer in the simulations was set to match that of DNA in 4 M LiCl (30 nm, 6σ).[5,6] The drag coefficient ζ, although not a fundamental unit, was also set to unity.

Geometry

For these simulations we modelled a filter pore as a cylindrical hole with WCA interactions creating an effective pore in the membrane. Although the domain of the simulation is unbounded, a hemisphere of radius 3Rg centered at the mouth of the pore, as shown in Figure S2, prevented the center of mass from diffusing any further. We kept the effective thickness of the pore fixed at 10σ (50 nm) to match experiment and varied the radius in the range $4\sigma \leq r_p \leq 10\sigma$. A caveat of this approach is that the simulated pores have circular cross sections rather than the various different cross sections present in the nanofilter pore distribution. The pore diameters used in the simulations correspond to pore major axis lengths in the experiment.

Simulation procedure

In the diffusive mode of operation, no electric field is applied to the system, so DNA strands that escape during the trapping time do so via unbiased translocation. Such events occur rarely, even for polymers very close to the nanopore. As such, we considered the question: given a polymer that has diffused near a filter pore, what is the probability that it will translocate through that pore before diffusing a significant distance away?

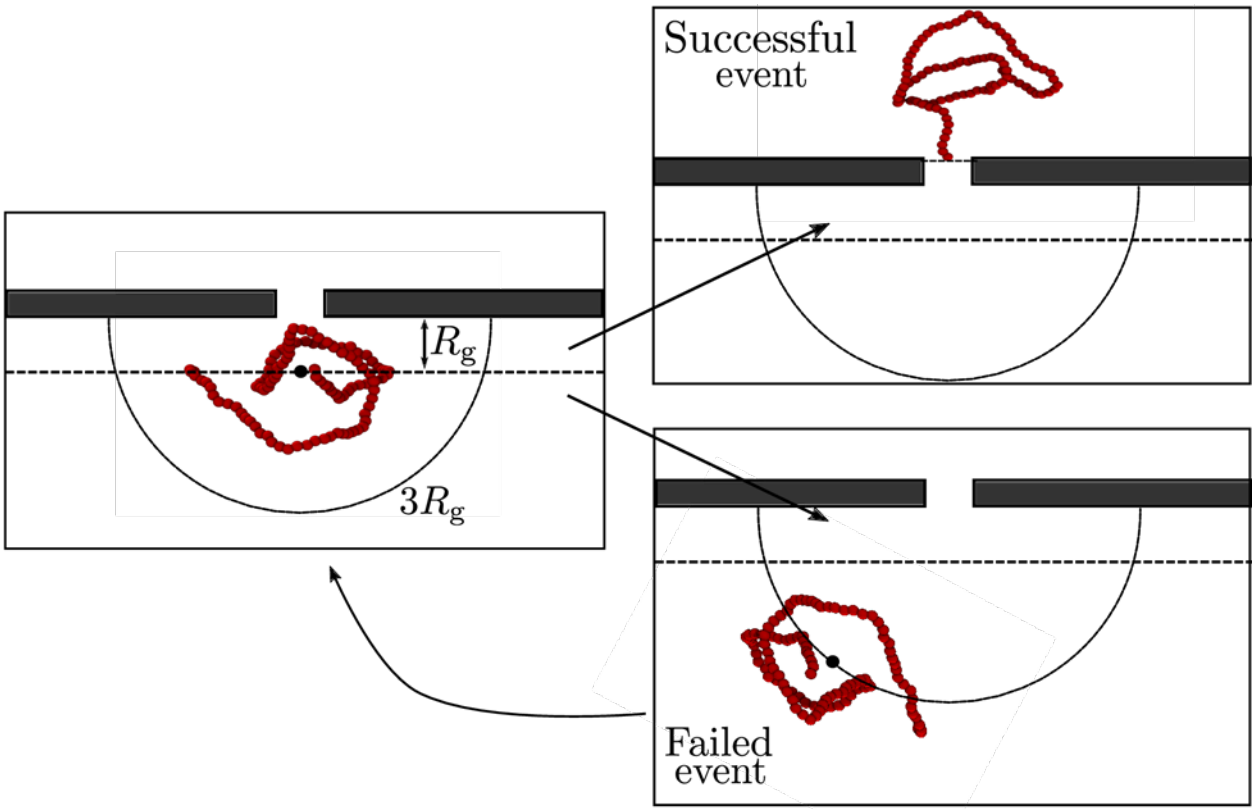

Figure S3: Schematic of the simulation geometry and procedure. The black dot represents the center of mass of the polymer. The black dashed line represents the initial distance from the pore membrane, and the black solid line represents the cutoff distance for the COM.

To compute these probabilities polymers were initialized with their center of mass on a disk that is R_g away axially from the mouth of the pore. The polymer either successfully translocates, classifying the event as a success, or diffuses away. An event was considered to have failed when the center of mass of the chain diffused further than $3R_g$ radially from the mouth of the pore.

At initialization the polymers should have equilibrium conformations, as prior to approaching the filter there is ample time to fully equilibrate. In the simulations the equilibration of a chain takes a considerable amount of computational time. Given that we expect a lot of failed

events, equilibrating the chain in the same simulation as the translocation events would quickly render the problem computationally infeasible. As such, we generated a database of five thousand equilibrium conformations that were used for initializing the polymers.

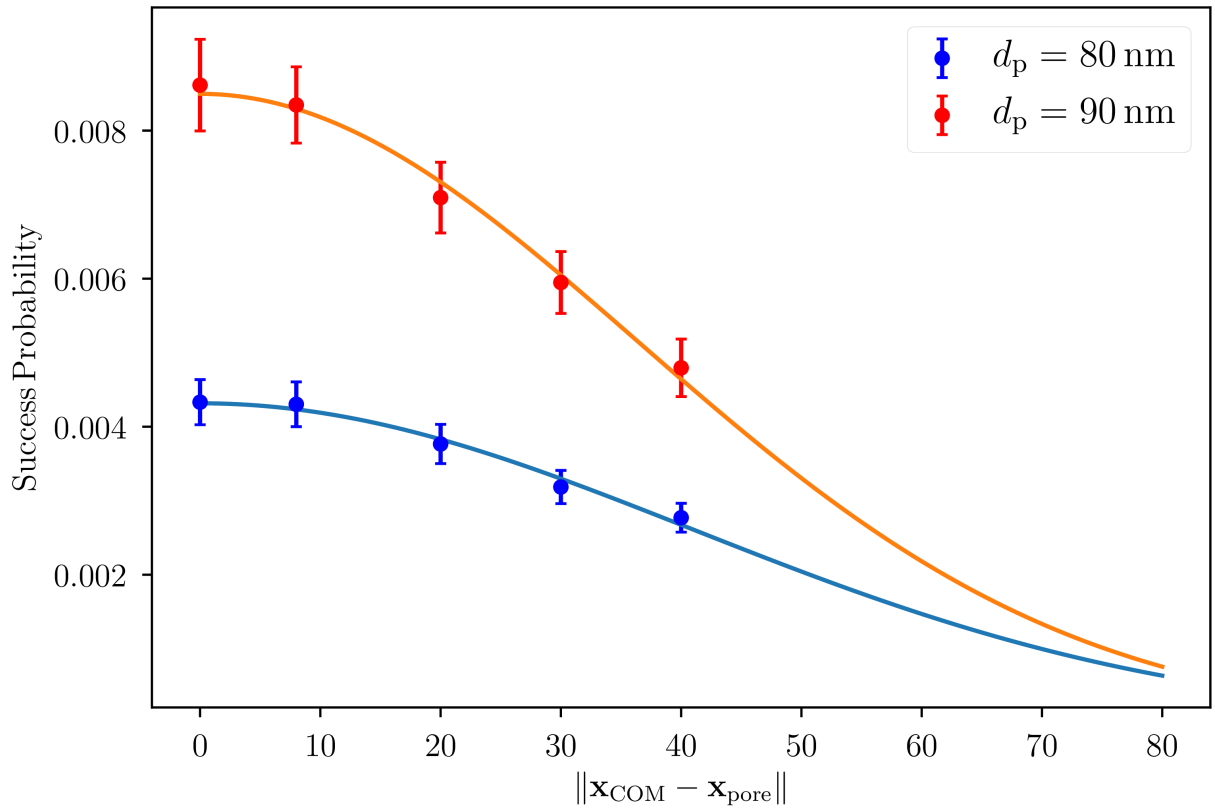

Figure S4: Success probability as a function of initial distance from the central axis of the nanopore to the COM. The solid lines are the fits to the data. The fit parameters can be found in Table S1.

When feasible, simulations were run for two hundred successful events for all pore radii. However, given the infrequency of successful events at smaller pores that was not always possible. As such, instead of running for a set number of successful events, some pore sizes were run for a

set number of failures, as displayed in Figure 4 of the main text. The probability of escape through the pore was computed as the number of successful events divided by the total number of events,

$$P_e = \frac{n_{successes}}{n_{failures} + n_{successes}} \tag{12}$$

As shown in Figure S4, we found that as we varied the initial axial offset of the COM on the disk, the variations in the probabilities were well fit by a Gaussian function of the form

$$p_{fit}(r) = a_0 \exp\left[\left(\frac{r}{a_1}\right)^2\right], \tag{13}$$

where a_0 and a_1 are fit parameters, shown in the Table S1. Note that for diameters of 70 and 100 nm, we only changed a_0 to be the on-axis probability and did not change a_1. As a result, when coupling CGLD to BD, we were able to compute the probability of escape through a pore after the COM had interacted with any point in a disk around the pore. It was this result that led to our choice for the disk radius described in the preceding section.

Table S1: Fit parameters for the success probability.

$\sigma = 5$ nm		
d_p (nm)	a_0	a_1
70 (*)	0.00295832	1.44520178
80	0.00431574	1.44520178
90	0.00849688	1.28618592
100(*)	0.01259953	1.28618592

The half-life of M13

Simulations were also used to gain some insight on the effectiveness of the nanofiltered nanopore device as a trap for M13. Given the size of M13 (7 kbp), conducting similar simulations to those described in the preceding sections would be infeasible. As a result, instead of simulating M13, we simulated the longest chains we feasibly could and extrapolated to obtain a conservative estimate of the trapping time for M13.

With the length scale chosen for the model described in the previous sections simulating polymers longer than 2 kbp becomes computationally challenging as the number of monomers becomes very large. As such, we modified the length correspondence by choosing the monomer size to be σ = 10 nm. The most salient effect of this change is that all the lengths in simulation units were halved, including the effective dimensions the nanopore. Given that all the simulations lengths were modified, we repeated the CGLD simulations explained in the previous section to obtain the probabilities of translocation, as shown in Figure S5.

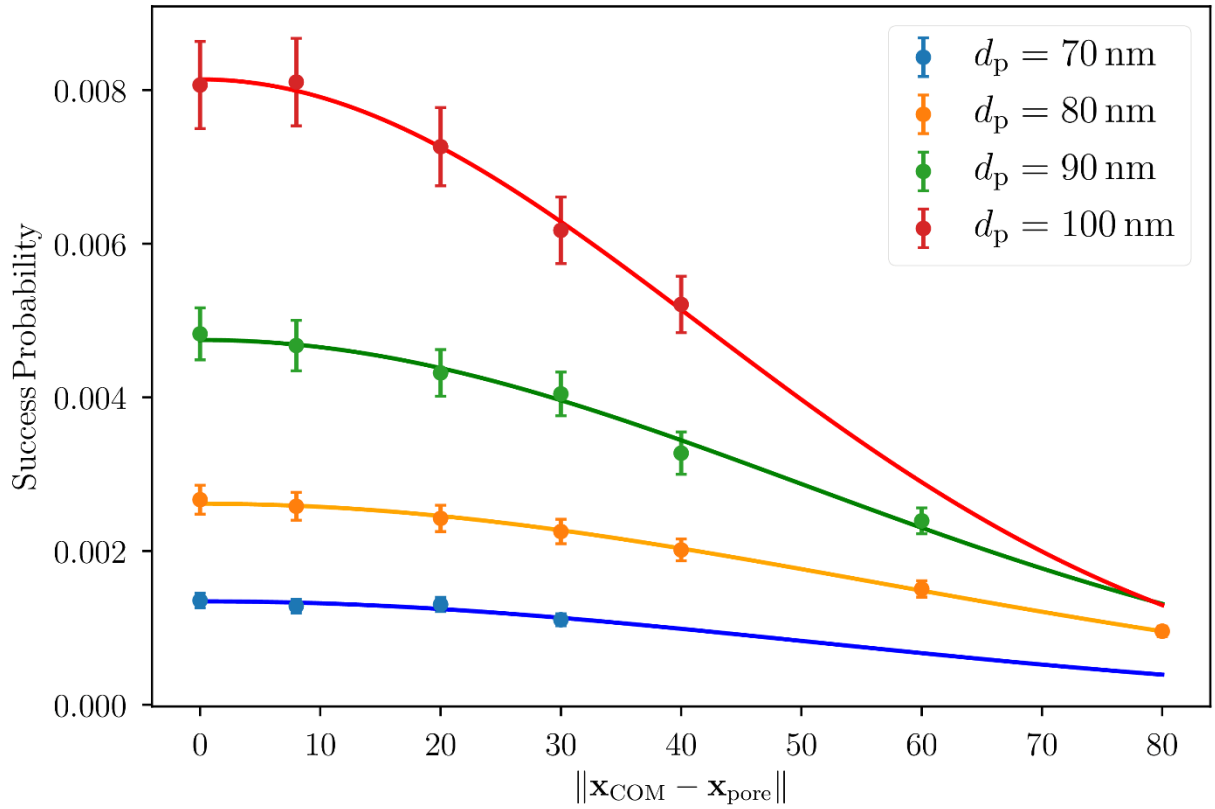

Figure S5: Success probability for a different length correspondence to Figure S4.

Table S2: Fit parameters for the success probability using $\sigma = 10$ nm.

d_p (nm)	a_0	a_1
70	0.00134558	1.79900229
80	0.00261617	1.99259571
90	0.00474791	1.76365758
100	0.00813947	1.47562624

The different length correspondence allowed us to use CGLD to simulate longer chains. Using the methodology described in the previous section we conducted BD simulations for 1.2 kbp, 1.5 kbp, 2.2 kbp, 2.9 kbp, and 3.7 kbp.

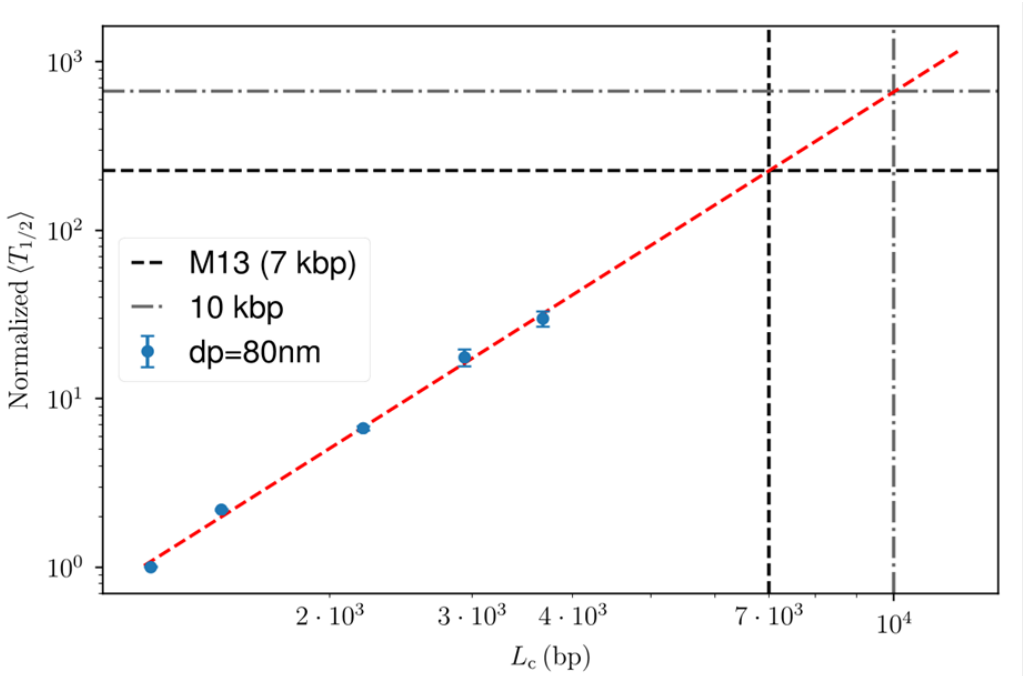

Figure S6: Normalized time for half the molecules to escape the device. The values are normalized by the value at L_c = 1.2 kbp as that is the only value for which both experimental and simulation results are available. The red dashed line is a power law fit to data with the exponent being 3.0238.

Figure S6 shows the half-life is well fit by a power law at the polymer lengths simulated. By extrapolating the fit to the length of M13 and 10 kbp we estimated the half-life to be 230 and 670 times longer than that of 1.2 kbp, respectively. Given that the half-life for 1.2 kbp is around 10 seconds, the half-life for M13 would be ≈40 minutes. This estimated time is in agreement with the experimental results, where virtually no escape events were recorded within 30 seconds of waiting.

Supporting Information Section S2: Effective Pore Diameter Distribution

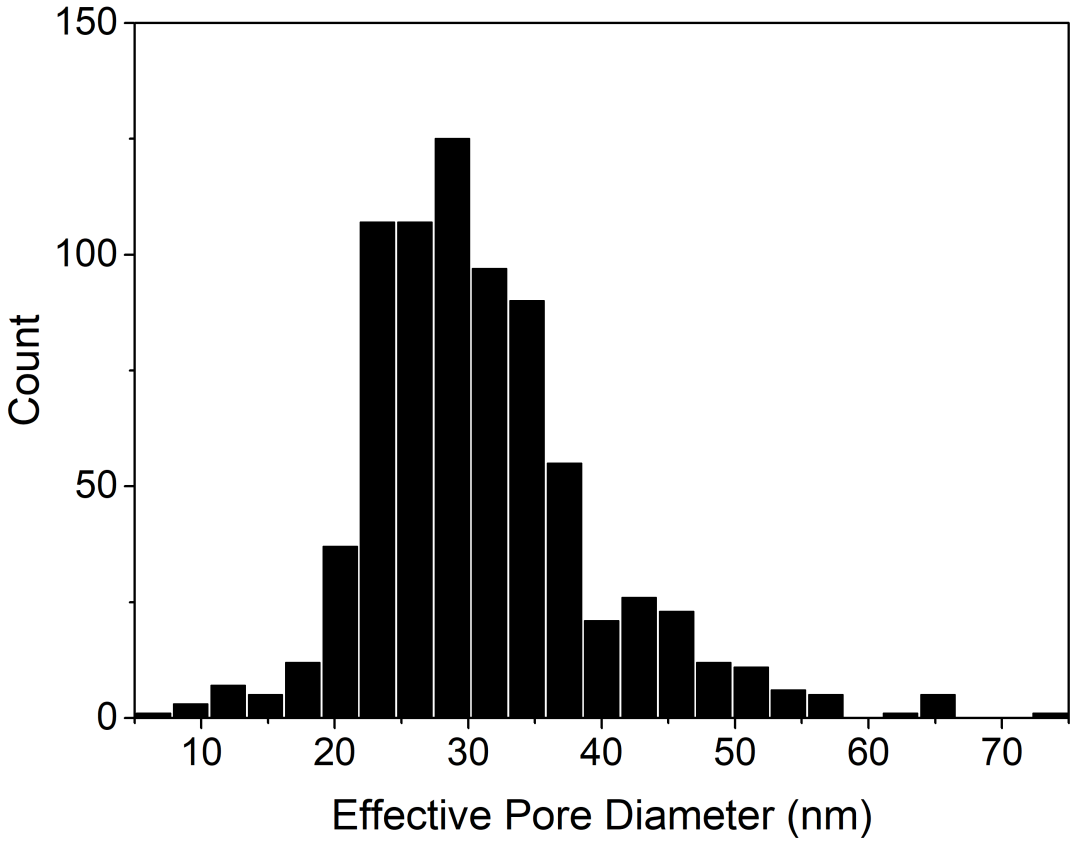

Figure S7: The distribution of effective pore diameter distribution, estimated as the geometric mean of the major and minor axes of the fitting ellipse.

Supporting Information Section S3: Additional Event Traces

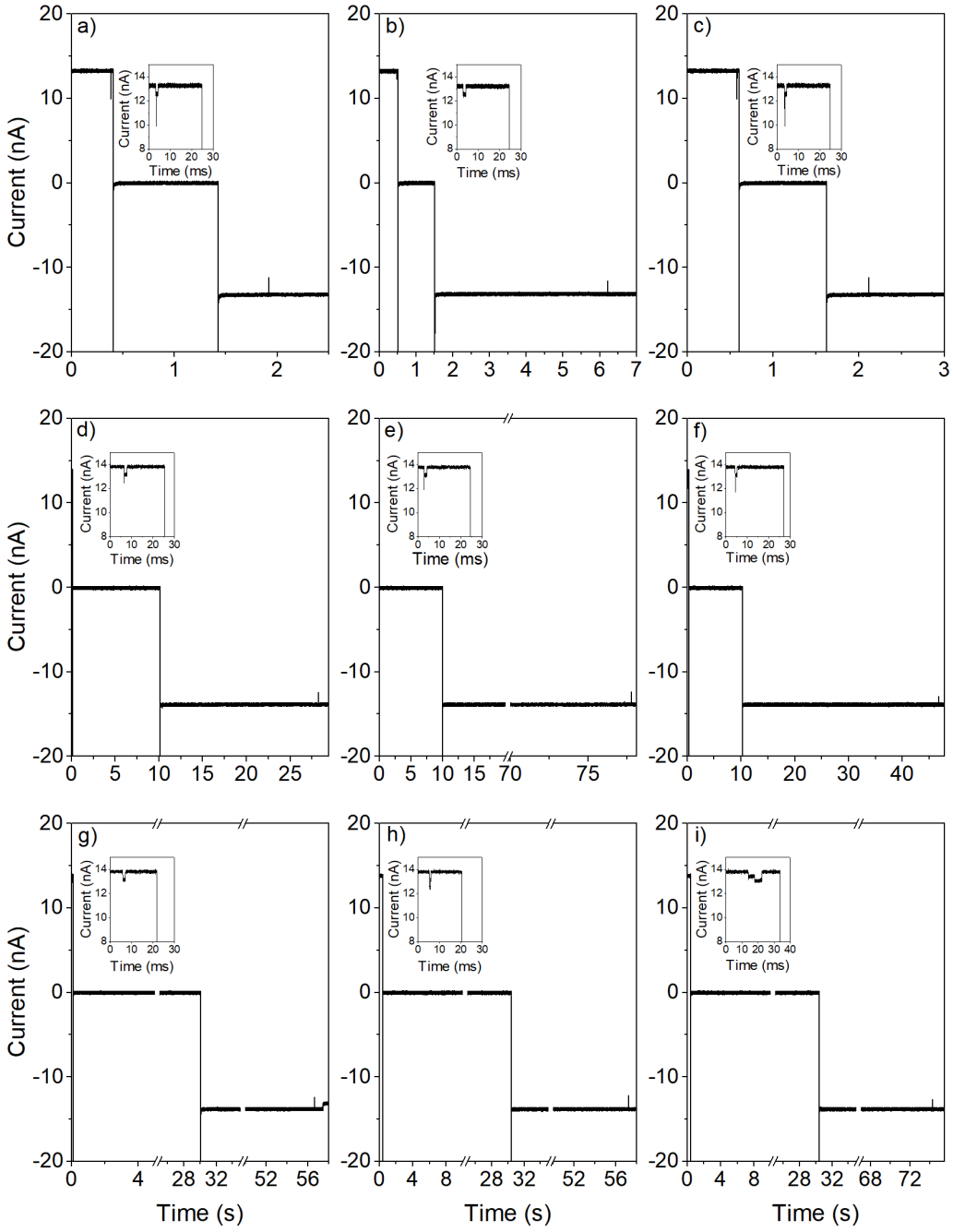

Figure S8: Additional single-molecule 10 kbp DNA trapping events in the diffusive mode for (a-c) 1s delay times, (d-f) 10s delay times, and (g-i) 30s delay times using Device C from the main text. Insets show the loading events. Note axis breaks in some cases where delay times are long.

References

(1) Petrov, E. P.; Ohrt, T.; Winkler, R. G.; Schwille, P. Diffusion and Segmental Dynamics of Double-Stranded DNA. *Phys. Rev. Lett.* **2006**, *97* (25), 258101. https://doi.org/10.1103/PhysRevLett.97.258101.

(2) Slater, G. W.; Holm, C.; Chubynsky, M. V.; de Haan, H. W.; Dube, A.; Grass, K.; Hickey, O. A.; Kingsburry, C.; Sean, D.; Shendruk, T. N.; et al. Modeling the Separation of Macromolecules: A Review of Current Computer Simulation Methods. *Electrophoresis* **2009**, *30* (5), 792–818. https://doi.org/10.1002/elps.200800673.

(3) Grest, G. S.; Kremer, K. Molecular Dynamics Simulation for Polymers in the Presence of a Heat Bath. *Phys. Rev. A* **1986**, *33* (5), 3628–3631. https://doi.org/10.1103/PhysRevA.33.3628.

(4) Landau, L. D.; Lifshitz, E. M.; Sykes, J. B.; Reid, W. H. Course of Theoretical Physics. In *Vol. 7 Theory of Elasticity*; Elsevier, 2013.

(5) Sobel, E. S.; Harpst, J. A. Effects of Na+ on the Persistence Length and Excluded Volume of T7 Bacteriophage DNA. *Biopolymers* **1991**, *31* (13), 1559–1564. https://doi.org/10.1002/bip.360311311.

(6) Savelyev, A. Do Monovalent Mobile Ions Affect DNA's Flexibility at High Salt Content? *Phys. Chem. Chem. Phys.* **2012**, *14* (7), 2250. https://doi.org/10.1039/c2cp23499h.